# A Concerted Synthetic, Spectroscopic, and Computational Approach towards Water Splitting by Homo- and Hetero-metallic Complexes

**Cláudio N. Verani, H. Bernhard Schlegel, John F. Endicott**

Department of Chemistry, Wayne State University, Detroit, MI 48202

## Introduction and Objectives Catalysis:

**Overview.** A comprehensive effort is under development at Wayne State University aiming at proton/water reduction by modular supramolecular multimetallic complexes. Such complexes can incorporate reactive sites, and antennae capable of accumulating and shuttling multiple electrons. In order to proceed, we are employing synthetic, redox-, spectroscopic-, surface-, and computation-based techniques to understand photo induced-electron transfer, charge separation, and efficient dihydrogen production in bulk and on surfaces..

**Long-term Objectives.**

(i) Development of integrated photoactive systems with antenna / active site for H2 production from organic acid / water; (ii) development of new electro- and photocatalysts for efficient proton-reduction.

**Current Objectives.**

(i) Design of robust catalysts that could retain their molecular nature under catalytic conditions.

(ii) Integration of these electrocatalytic modules with photosensitizers to form heterobimetallic photocatalysts.

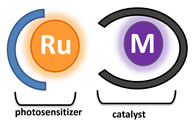


## Cobalt/Oxime Frameworks :

### Mechanistic Insights into Proton Reduction using Cobalt Oximes

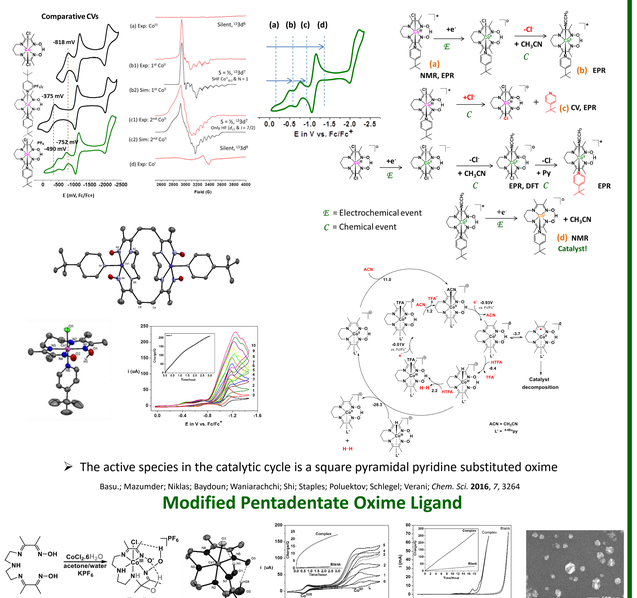


➢ The active species in the catalytic cycle is a square pyramidal pyridine substituted oxime

Basu.; Mazumder; Niklas; Baydoun; Waniarachchi; Shi; Staples; Poluektov; Schlegel; Verani; *Chem. Sci.* **2016**, *7*, 3264

### Modified Pentadentate Oxime Ligand

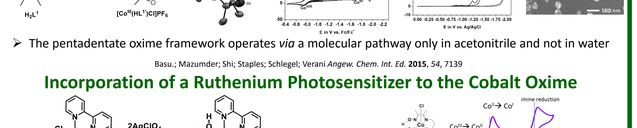


➢ The pentadentate oxime framework operates *via* a molecular pathway only in acetonitrile and not in water

Basu.; Mazumder; Shi; Staples; Schlegel; Verani *Angew. Chem. Int. Ed.* **2015**, *54*, 7139

### Incorporation of a Ruthenium Photosensitizer to the Cobalt Oxime

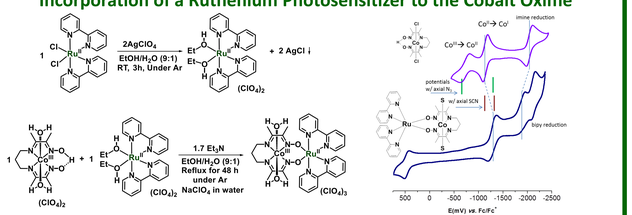


➢ A Ru-Co dyad can be obtained by using the oxime oxygens as linkers

### Spectroscopic Comparison

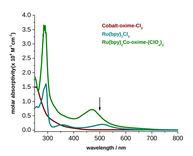


### Comparative Electrocatalytic Activity

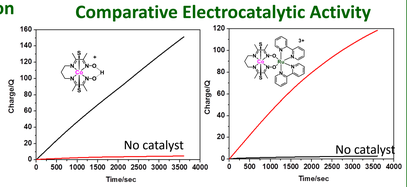


● Overpotential: 0.36 V
TON: 17.8 (3 h, ACN)

● Overpotential: 0.39 V
TON: 17.0 (3 h ACN)

➢ Electrocatalytic activity is retained after three hours of catalysis

### [Co^III Ru^II]: Photocatalytic Activity

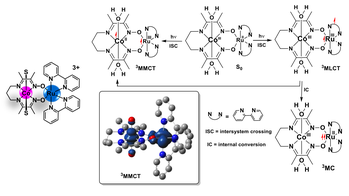


● Three possible triplet excited states. 3MMCT is feasible Mulliken spin density of 1.04 and 0.86 for $^{LS}Co^{II}$ and $Ru^{III}$ respectively.

● $Ru^{II}Co^{III} \rightarrow Ru^{III}Co^{II}$ is energetically favorable, but not sufficient to reach the $Co^{I}$ catalyst

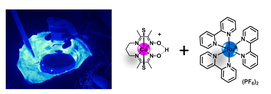

● TON = 65, 1 h
$Et_3N$: sacrificial donor
Aqueous acetate buffer, pH 4

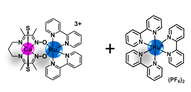

● TON 120, 3 h
$Et_3N$: sacrificial donor
Aqueous acetate buffer, pH 4

➢ The dyad has a significantly improved TON when compared to the monometallic cobalt oxime


## Cobalt/Nickel Pyridine Frameworks:

### Cobalt pyridine framework

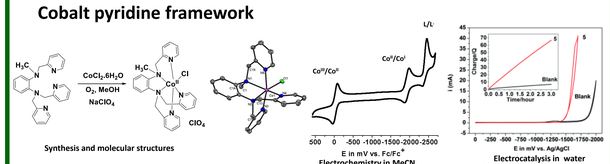


### Nickel pyridine framework

Basu.; Mazumder; Shi; Baydoun; Niklas; Poluektov; Schlegel; Verani; *Angew. Chem. Int. Ed.* **2015**, *54*, 2105

### Synthesis and Molecular Structures

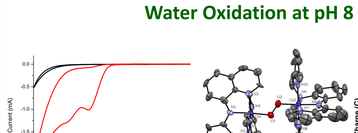


### Electrochemistry in MeCN

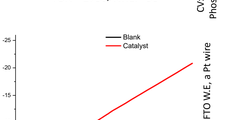


CV/TBAPF$_6$/Glassy C(WE), Ag/AgCl (RE), Pt-wire (AE)

### Electrocatalysis

**Electrocatalysis in water**

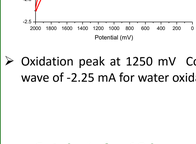


➢ Onset overpotential : 0.78 V
➢ TON: 1050 (3 h); FE: 96 %

**UV-Visible spectroscopy in phosphate buffer**

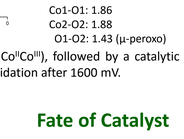


➢ The UV-Visible spectrum changed considerably after catalysis; suggesting that the catalyst is chemically altered.

**SEM and EDAX**

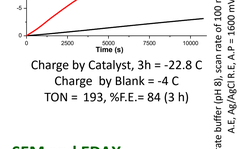


➢ SEM: No visible nanoparticle formation on the grafoil electrode. EDS: %Ni = 0 on grafoil electrode
➢ SEM and EDS: The Ni catalyst is molecular in nature after 8 h catalysis

### Photocatalysis

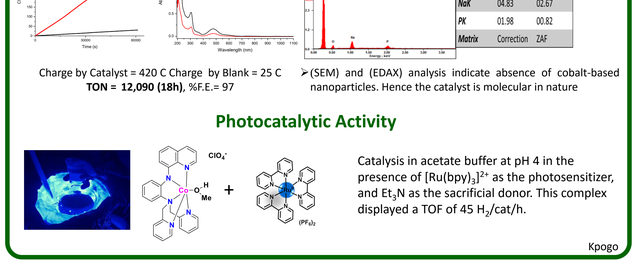


➢ Total TONs of $H_2$ production after 48 h at different pH values.
➢ Variation from pH 10-14 revealed optimal performance at pH 12
➢ Total TONs of $H_2$ production after 24 h with varying amounts of the Ni complex.
➢ Catalyst concentration and TON vary inversely: Maximum TON (3500) was achieved for the system with the minimum Ni catalyst concentration




## Cobalt/Quinoline Frameworks:

### Synthesis and Molecular Structure




### Water Reduction at Neutral pH

**Electrochemistry in MeCN**




•$Co^{III}$/ $Co^{II}$ $E_{1/2}$ = 0.45 V $_{Fc+/Fc}$
•$Co^{II}$/ $Co^{I}$ E = -1.03 V $_{Fc+/Fc}$

**Catalytic Current Enhancement**




Overpotential: 0.65V

**Catalysis for three hours**




Charge by Catalyst = 120C
Charge by Blank = 8C
TON = 2730, %F.E.= 98

CV: Complex (0.25 X $10^{-3}$M)/Water/Phosphate buffer/pH:7; BE (Wate Phosphate buffer (20 mL)/pH-7/Hg-pool (WE), Ag/AgCl (RE), Pt-coil (A 1700 mV Vs. Ag/AgCl/ Complex (0.2 umol)

### Water Oxidation at pH 8




➢ Oxidation peak at 1250 mV $Co^{II}Co^{III}$), followed by a catalytic wave of -2.25 mA for water oxidation after 1600 mV.

Charge by Catalyst, 3h = -22.8 C
Charge by Blank = -4 C
TON = 193, %F.E.= 84 (3 h)

### Fate of Catalyst

**Catalysis for 18 hours**




**SEM and EDAX**



| Element | Wt % | At % |
|---|---|---|
| CK | 86.59 | 91.28 |
| OK | 06.60 | 05.24 |
| NaK | 04.83 | 02.67 |
| PK | 01.98 | 00.82 |
| Matrix | Correction | ZAF |

Charge by Catalyst = 420 C Charge by Blank = 25 C
**TON = 12,090 (18h)**, %F.E.= 97

➢ (SEM) and (EDAX) analysis indicate absence of cobalt-based nanoparticles. Hence the catalyst is molecular in nature

CV 0.1M borate buffer (pH 8), scan rate of 100 mVs$^{-1}$ FTO W.E., a Pt wire A.E, Ag/AgCl R.E, A.P = 1600 mV

### Photocatalytic Activity




Catalysis in acetate buffer at pH 4 in the presence of $[Ru(bpy)_3]^{2+}$ as the photosensitizer, and $Et_3N$ as the sacrificial donor. This complex displayed a TOF of 45 $H_2$/cat/h.

Kpogo

## Cobalt /Amide Frameworks for Water Reduction:

### Synthesis

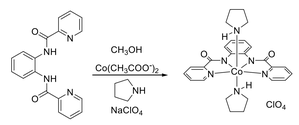


➢ The bis-amido ligand and cobalt complex can be readily synthesized at multigram scales

### Electrochemistry in MeCN

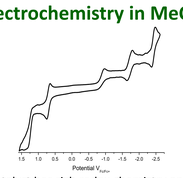


➢ The catalyst has rich redox chemistry and can stabilize Co(I) at -1.7 $V_{Fc/Fc+}$

### Electrocatalysis in Neutral Water

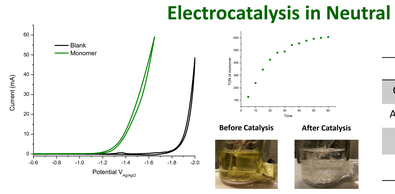


| | Monomer |
|---|---|
| Concentration (μmol.L$^{-1}$) | 8 |
| Applied Potential ($V_{Ag/AgCl}$) | -1.41 |
| TON based on cobalt | 670 (1h) |
| Faradaic Efficiency (%) | 97 |

### Structural and Spectral Properties Upon Reduction

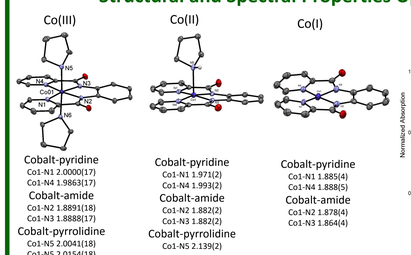


➢ Negligible bond length changes on ligand indicate the absence of radical in the solid state
➢ Absorption peak in the Near-IR region indicates presence of radical in the Co(I) state
➢ Implies in an equilibrium between the metal-centered and the ligand-centered reductions

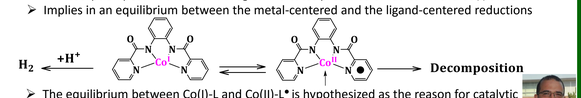


➢ The equilibrium between Co(I)-L and Co(II)-L• is hypothesized as the reason for catalytic instability


## Bimetallic Cobalt Frameworks for Proton Reduction:

### Synthesis and Molecular Structures

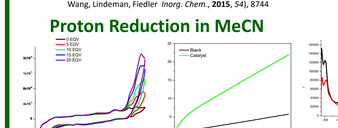


Wang, Lindeman, Fiedler *Inorg. Chem.*, **2015**, 54), 8744

• $(LF^{Me})^{3-}$ ligand supports a dicobalt(II) core bridged by a diarylamido unit.
•Each Co(II) is five-coordinate

### Fate of Catalyst

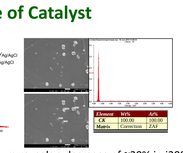


### Proton Reduction in MeCN




•$[Co^{II}\text{-}Co^{II}]/[Co^{II}\text{-}Co^{I}]$ = -1.45 V $_{Fc+/Fc}$
•$[Co^{II}\text{-}Co^{I}]/[Co^{I}\text{-}Co^{I}]$ E = -1.86 V $_{Fc+/Fc}$

Charge by Catalyst = 22C
Charge by Blank = 6C
TON = 18, %F.E.= 94

➢ Post-catalysis spectrum reveals a decrease of ~30% in i300 nm band and ~ 10% decrease in 450 nm band: bipy detach.
➢ SEM and EDAX analyses indicate that nanoparticles are not cobalt-based, ergo not catalytically active.

### Catalytic Mechanism Involves Two Cobalt Centers

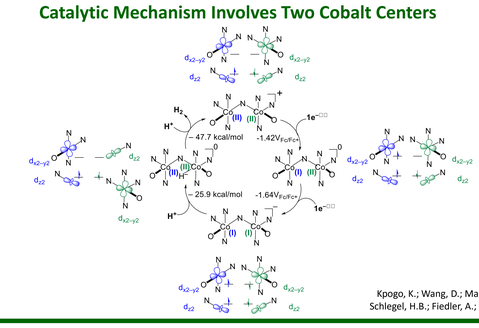


Kpogo, K.; Wang, D.; Mazumder, S.; Schlegel, H.B.; Fiedler, A.; Verani, C.N.

## Heterogeneous Water Oxidation

### Film Formation

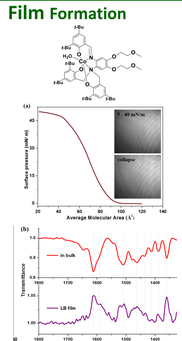


### Electrocatalysis at pH 11

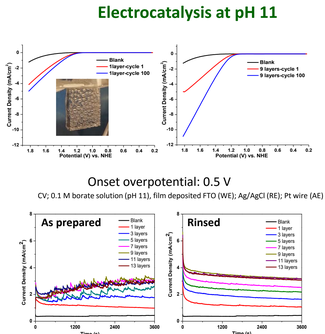


Onset overpotential: 0.5 V
CV; 0.1 M borate solution (pH 11), film deposited FTO (WE); Ag/AgCl (RE); Pt wire (AE)




➢ Using the Langmuir-Blodgett method FTO electrodes can be modified in a layer by layer fashion
➢ The precursor molecular films rearrange on the surface of the electrode
➢ The estimated TOF for a monolayer is 54000 ± 1500 $h^{-1}$

Gonawala.; Baydoun; Wickramasinghe; Verani; *Chem. Commun.*. 2016, *Accepted*




## Visible Light Photodecomposition of Redox Active Sensitizers

### Near UV irradiation of $[Ru(bpy)_3]^{2+}$ produces solvated electrons in a sequential absorption of two photons[1]

$Ru(bpy)_3^{2+} + h\nu_{abs} \rightarrow \ldots \rightarrow {}^3MLCT$ $(\phi_a I_a)$ with 532 nm laser

${}^3MLCT \rightarrow Ru(bpy)_3^{2+} + h\nu_{em}$ $(k_{RAD})$

${}^3MLCT \rightarrow Ru(bpy)_3^{2+} + heat$ $(k_{NDR})$

**$^3MLCT + h\nu_{abs*} \rightarrow Ru(bpy)_3^{3+} + e^-_{(solv)}$** **$(\phi_e I_e)$ with 405 nm laser**

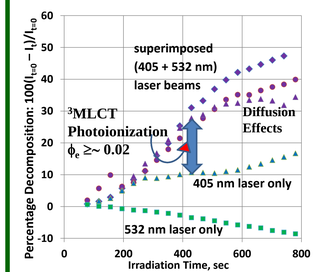


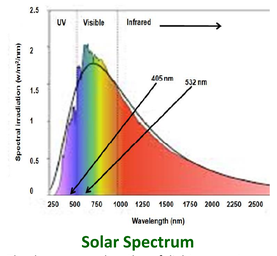


### $^3$MLCT Photoionization:

Ambient aqueous solution; 0.5 M HOTf (e$^-$(solv) scavenger); 0.1 M 2-propanol (H-atom scavenger); $10^{-4}$ M $Ru(bpy)_3^{2+}$; (50 & 80 mW cw 405 & 532 nm lasers)

### Solar Spectrum

The longer wavelengths of light generate an excited state that absorbs light in the solar spectral regime and is photoionized: simulated by 532 and 405 nm irradiations, respectively

Two-Photon photoionization of redox active molecules depends on: (1) donor ionization energy (or oxidation potential); (2) transient excited state energy, absorption spectrum and lifetime; (3) possibly a reorganizational energy (being investigated).

1. Goez; Von Ramin-Marro; Musa; Schiewek; *J. Phys. Chem. A* 2004, 108, 1090


## Observations on Ru-Aromatic Ligand $^3$MLCT Emission Spectra

### We have found that:

The relative amplitudes of vibronic sidebands in Ru-bpy chromophores increase as the excited state energy increases

Xie; Chen; Uddin; Endicott; *J. Phys. Chem. A* **2004**, *109*, 4671
Odongo; Heeg; Chen; Xie; Endicott; *Inorg. Chem.* **2008**, *47*, 7493
Lord; Allard; Thomas; Odongo; Schlegel; Chen; Endicott; *Inorg. Chem.* **2013**, *52*, 1185




### Comparison of Observed and Calculated $^3$MLCT Emission Band Shapes

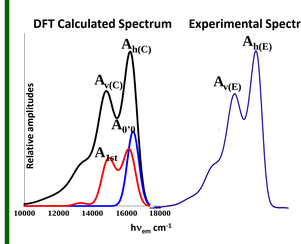


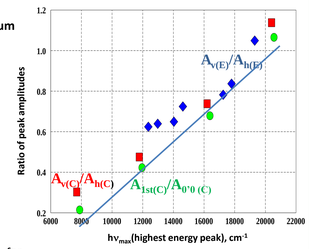


DFT-calculated and observed emission spectra for $[Ru(NH_3)_4bpy]^{2+}$; the DFT-calculated band origin and sum of progressions in distortion mode harmonics are shown.

Excellent agreement: but the calculated vibronic structure arises from configurational mixing in the triplet manifold.

### Configurational Mixing in $^3$MLCT Emissive State: Ru-bpy vs. Ru-MDA Chromophores

$k_{RAD} = \phi_{em}/\tau_{obsd}$

$k_{RAD}$ increases more strongly with energy than expected (intensity stealing) for Ru-bpy chromophores but not for Ru-MDA chromophores. (MDA = mono-dentate aromatic; e.g., py, pz, ...)

The intensity of the $^3$MLCT emissions depends on spin-orbit coupling promoted mixing between it and excited states in the singlet spin manifold; possibly ($^3$MLCT + $^3\pi\pi^*$)/$^1$MLCT or $^3$MLCT/$^1\pi\pi^*$.

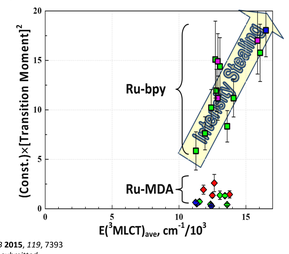


Thomas; Tsai; Mazumder; Lu; Lord; Schlegel; Endicott; Chen; *J. Phys. Chem. B* **2015**, *119*, 7393
Tsai; Mazumder; Zhang; Schlegel; Chen; Endicott; *Inorg. Chem.* **2016**, *submitted*

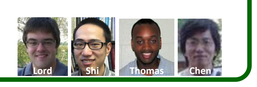


## Acknowledgements

Office of Basic Energy Sciences
DE-SC001907, DE-FG02-09ER16120